Electronic Supplementary Material (ESI) for Medicinal Chemistry Communications.

SUPPORTING INFORMATION

Stabilization for Loop Isomers of C-Myc G-Quadruplex DNA and Anticancer Activity by Ruthenium Complexes

Ying Liu, [a†] Yanan Liu, [b†] Licong Yang, [a] Chengwen Cao, [a] Yanhui Zhou [a] and Jie Liu[*a]

[a] Department of Chemistry, Jinan University, Guangzhou 510632, China.

[b] School of Life Sciences and State Key Laboratory of Agrobiotechnology, The Chinese University of Hong Kong, Hong Kong SAR.

Experimental section

Reagents and Materials: All chemicals were obtained from commercial sources unless otherwise specified, and Ultrapure MilliQ water (18.2 MΩ) was used in all experiments. c-myc DNA Pu27 (5'-TGGGGAGGGTGGGGAGGGTGGGGAAGG-3') and Pu18 (5'-AGGGTGGGGAGGGTGGGG-3') were purchased from Shanghai Sangon Biological Engineering Technology & Services (Shanghai, China). The concentration of c-myc DNA was determined by measuring the absorbance at 260 nm after melting. The formations of intramolecular G-quadruplex was carried out as follows: the oligonucleotide samples, dissolved in different buffers, were heated to 90℃ for 5 min, spontaneously cooled to room temperature, and then incubated at 4 ℃ overnight. Buffer A: 10mM Tris-HCl, pH=7.4; Buffer B: 10 mM Tris-HCl, 100 mM KCl, pH=7.4; Buffer C: 1.5 mM Na_2HPO_4, 0.5 mM NaH_2PO_4, 0.25 mM Na_2EDTA. Further dilution was made in the corresponding buffer to the required concentrations for all the experiments.

Physical measurement: Elemental analyses (C, H, and N) were carried out with a Perkin-Elmer 240C elemental analyzer. ^{1}H NMR spectra were recorded on a Varian Mercury-plus 300 NMR spectrometer with [D_6]DMSO as solvent and $SiMe_4$ as an internal standard at 300 MHz at room temperature. Electrospray ionization mass spectrometry (ES-MS) was recorded on a LQC system (Finngan MAT, USA) by using CH_3CN as a mobile phase. Emission spectra was recorded on a Perkin-Elmer Lambda-850 spectrophotometer. The CD spectra was recorded on a Jasco J-810 spectropolarimeter.

Synthesis of ligands and complexes: Ruthenium (III) chloride hydrate was purchased from Alfa Aesar; 1,10-Phenanthroline-5,6-dione and $dhipH_3$ (3,4-dihydroxyl-imidazo[4,5-*f*][1,10]phenanthroline) were obtained from Sigma. cis-[$Ru(bpy)_2Cl_2$]·$2H_2O$ and cis-[$Ru(phen)_2Cl$]·$2H_2O$ were prepared and characterized according to the literature.[1] ($dhipH_3$) was also prepared according to the literature.[2]

Synthesis of [$Ru(bpy)_2(dhipH_3)](ClO_4)_2$ (1): A mixture of 0.63 g (3 mmol) of 1,10-phenanthroline-5,6-dione, 0.41 g (3 mmol) of 3,4-dihydroxy-benzaldehyde, and 1.54 g (60 mmol) of ammonium acetate dissolved in 50 mL of EtOH was refluxed at 85 ℃ for 6 h under the protection of nitrogen and then was cooled to room temperature. A light yellow precipitate was vacuum filtrated and was recrystalized from N,N-dimethylformamide and CH_2Cl_2. The light yellow solid was collected and dried under vacuum, then purified by column chromatography on alumina with acetonitrile/toluene (4:1 v/v) as eluent. The solvent was removed under reduced pressure and red microcrystals were obtained; yield : 0.148 g, 49.6 %. ^{1}H-NMR (DMSO-d_6, dppm): 9.20 (d, 2H), 8.90 (dd, 4H), 8.22 (t, 2H), 8.11 (t, 2H), 8.00 (d, 2H), 7.86 (dd, 2H), 7.61 (t, 4H), 7.35 (t, 2H); ES-MS of the ClO_4 salt in CH_3OH: m/z 741.3 $[M\text{-}2ClO_4]^+$, 371.4 $[M\text{-}2ClO_4]^{2+}$; elemental analysis calcd (%) for $C_{39}H_{28}N_8Cl_2O_{10}Ru$: C 49.79, H 2.98, N 11.91; found: C 49.80, H 2.97, N 11.90(Fig. S11).

Synthesis of [$Ru(phen)_2(dhipH_3)](ClO_4)_2$ (2): This complex was synthesized in a manner identical to that described for [$Ru(bpy)_2(dhipH_3)](ClO_4)_2$ (**1**), with cis-[$Ru(phen)_2Cl_2$]·$2H_2O$ (0.17 g, 0.3 mmol) in place of cis- [$Ru(bpy)_2Cl_2$]·$2H_2O$; yield : 0.175 g, 56.0 %. ^{1}H-NMR (DMSO-d_6, dppm): 9.07 (d, 2H), 8.78 (dd, 4H), 8.40 (t, 2H), 8.14 (t, 2H), 8.04 (d, 2H), 7.96 (dd, 2H), 7.92 (d, 2H), 7.78 (t, 4H); ES-MS of the ClO_4 salt in CH_3OH: m/z 788.3 $[M\text{-}2ClO_4\text{-}2H]^+$, 395.4 $[M\text{-}2ClO_4]^{2+}$; elemental analysis calcd (%) for $C_{43}H_{28}N_8Cl_2O_{10}Ru$: C 52.23, H 2.83, N 11.34; found: C 52.24, H 2.82, N 11.33(Fig. S12).

Emission Titration: Solutions of the ruthenium(II) complexes (10 μM) were prepared in 10 mM Tris-HCl (pH 7.4) containing 100 mM KCl buffer and aliquots of 1-10 mL of Pu27 DNA solution (5-10 μM) were added.

Solutions of the ruthenium(II) complexes (5 μM) were prepared in 10 mM Tris-HCl (pH 7.4) containing 100 mM KCl buffer and aliquots of 1-10 mL of Pu18 DNA solution (0-20 μM) were added. The 18-mer sequences: (5'-AGGGTGGGGAGGGTGGGG-3')

c- myc 1:2:1 (G→T-14,23) (5'-AGGGTGGGTAGGGTGGGT-3')
c- myc 2:1:1 (G→T-11,23) (5'-AGGGTTGGGAGGGTGGGT-3')
c- myc 1:2:2 (G→T-14,20) (5'-AGGGTGGGTAGGGTTGGG-3')
c- myc 2:1:2 (G→T-11,20) (5'-AGGGTTGGGAGGGTTGGG-3')

Emission spectra were recorded in the λ = 500-780 nm range after equilibration at 20 ℃ for 10 min per aliquot until saturation point had been reached.[3,4]

The intrinsic binding constants for **1** and **2** were determined based on the emission enhancement according to the Scatchard equation (1), where C_t is the total compound concentration, F is the observed fluorescence emission intensity at a given DNA concentration, F_0 is the intensity in the absence of DNA, and F_{max} is the fluorescence of the completely bound compound.

$$C_b = C_t\,(F - F_0)/(F_{max} - F_0) \quad (1a)$$

$$r = C_b/C_{DNA} \quad (1b)$$

$$r/C_f = nK_b - rK_b \quad (1c)$$

Binding data was analyzed in the form of a Scatchard plot of r/C_f versus r, where r is the binding ratio of C_b/[DNA] and C_f is the free ligand concentration.

Circular dichroism measurements: CD spectra of the oligonucleotides were recorded on a Jasco J-810 spectropolarimeter.[5] A quartz cell of 1 mm optical path length and an instrument scanning speed of 100 nm/min with 1 s response time was used for measurements. The measurements are the averages of three repetitions between 200 and 400 nm at room temperature. Spectra were baseline-corrected and the signal contributions of the buffer were subtracted. 1.0 mL ruthenium(II) complexes (1 mM) were added sequentially to solutions containing Pu27 DNA (2.0 mM), respectively.

Fluorescence resonance energy transfer (FRET) studies: The fluorescent labeled oligonucleotide, F27T (5'-FAM-[$TG_4AG_3TG_4AG_3TG_4AAGG$]-TAMRA-3', The donor fluorophore was 6-carboxyfluorescein, FAM, and the acceptor fluorophore was 6-carboxytetramethylrhodamine, TAMRA.) used as the FRET probes was diluted in Tris-HCl buffer (10 mM , pH 7.4) containing KCl (0.2 mM) and then annealed by being heated to 92 ℃ for 5 min, followed by cooling slowly to room temperature overnight.[6] The assay was based on measurements of ligand induced stabilization on a fluorescently labelled quadruplex-forming oligonucleotide (F27T, 5'-FAM-[$(TG_4AG_3)_2$ TG_4AAGG]-TAMRA-3').[7] By using a total reaction volume of 25 μL, with labeled oligonucleotide (0.2 μM) and different concentrations of complexes.

The fluorescent labeled oligonucleotide, F18T (5'-FAM-[AGGGTGGGGAGGGTGGGG]-TAMRA-3') used as the FRET probes was diluted in Tris-HCl buffer (10 mM , pH 7.4) containing KCl (10 mM) and then annealed by being heated to 92 ℃ for 5 min, followed by cooling slowly to room temperature overnight. The assay was based on measurements of ligand induced stabilization on a fluorescently labelled quadruplex-forming oligonucleotide (F18T, 5'-FAM-[AGGGTGGGGAGGGTGGGG]-TAMRA-3'). By using a total reaction volume of 25 μL, with labeled oligonucleotide (2 μM) and ruthenium(II) complexes (10 μM).

A constant temperature was maintained for 30 s prior to each reading to ensure a stable value. Final analysis of the data was carried out using Origin Pro 8 data analysis.

PCR stop assay: The polymerase stop assay was performed as described previously.[8] In this experiment, 5'-to-3' primer extension by DNA Taq polymerase was interrupted and the final double-stranded DNA PCR product was not obtained.[9] Varying concentrations of **1** and **2** (0, 3, 6, 9, 12, 15 and 20 μM) were used and PCR products were separated via PAGE and stained with silver. The Pu27 and the corresponding complementary sequence Pu27rev were used. The Pu18 and the corresponding complementary sequence Pu18rev were used. The reactions were performed in 1 × PCR buffer that contained 10 μM of each pair of oligomers, dNTP (0.16 μM), Taq polymerase (2.5 U), and the indicated concentrations of the complexes. Reaction mixtures were incubated in a thermocycler at 94 ℃ for 3 min, followed by 30 cycles of 94 ℃ for 30 s, 58 ℃ for 30 s, and 72 ℃ for 30 s. Amplified products were resolved on 15 % nondenaturing polyacrylamide gels in 1 × TBE and stained with silver.

Cell culture: HeLa, HepG2 (human hepatocellular liver carcinoma), SW620 (colorectal adenocarcinoma), MCF-7 (human breast adenocarcinoma), A549 (human lung carcinoma) cells, and Hs68(Human foreskin fibroblast) cells were incubated with varying concentrations of Ru(II) for 48 h to investigate the antitumor potential of the Ru(II) complexes. The cell lines were maintained in cell culture media (RPMI-1640 medium) supplemented with fetal bovine serum (10 %), penicillin (100 UmL^{-1}), and streptomycin (100 $\mu g\ mL^{-1}$) at 37 ℃ under a humidified atmosphere with 5 % CO_2.

MTT assay: Cell viability was determined by measuring the ability of cells to transform MTT (3-(4,5-dimethyl-2-thiazolyl)-2,5-diphenyl tetrazolium bromide) to a purple formazan dye . MTT cell-viability assays were conducted in 96-well, flat-bottomed microtiter plates. Cells were seeded in a 96-well microplate at 2000 cells per well in growth medium solution (150 μL). Complexes **1-2** and cisplatin (positive control) were mixed with the growth medium. Drug-treated and untreated cells were incubated for 48 h at 37 ℃, 5 % CO_2 in a humidified incubator. MTT reagent was added to each well. The microplates were then reincubated at 37 ℃ in 5 % CO_2 for 4 h, prior to the addition of solubilization solution (10 % SDS in 0.01 M HCl). The microplates were further incubated for 12 h. Absorbances at $\lambda = 570$ nm were measured on a microplate reader. IC_{50} values (concentration required to reduce the absorbance by 50 % compared with the controls) for each complex were determined by the dose dependence of surviving cells after exposure to the ruthenium(II) complexes for 48 h.

Cellular Uptake Experiment: HeLa cells treated with 10 μM of **1** and **2** were investigated using flow cytometry to obtain the time-dependent uptake profiles.[10] Flow cytometry was used to test fluorescence intensity after cells were incubated for 4, 8 and 12 h at this concentration. HeLa cells in growth medium were seeded in 35 mm tissue culture dishes (Corning) and incubated at 37 ℃under a 5% CO_2 atmosphere until 70% confluent. The culture medium was removed and replaced with medium (final DMSO concentration, 1% v/v) containing the ruthenium(II) complexes at 10 μM . After incubation for 12, 24, 36 h respectively, the cell layer was trypsinized and washed twice with cold PBS (phosphate buffered saline). The samples were raised in 500 μL of cold PBS and analyzed by a BD FACSAria flow cytometer immediately. The samples were collected in FL2 channel (excitation at 488 nm and emission at 585 ± 21 nm), and the number of cells analyzed for each sample was 10000.[11]

Flow cytometric determination of cell cycle and apoptosis: HeLa cells (1×10^6 cells in each 60 mm petridish) were treated with various concentrations of ruthenium(II) complexes (0, 5, 10, 20 μM) for 48 h for cell cycle arrest and apoptosis. Cells were treated with **1** and **2** for 48 h then stained with PI (propidium iodide). Representative DNA distribution histograms of HeLa cells treated in the absence and presence of 5, 10 and 20 μM of **1** and **2**. For cell cycle analysis, the cells of each petridish were harvested with trypsin and fixed overnight in an ice cold 70% ethanol solution at -20 ℃ overnight. After centrifugation and further washing with PBS, cells were incubated with 200 μL 10 μg/mL PI and 0.5 mg/mL RNase A in PBS for 30 min at 37 ℃ in the dark. The data analysis was performed in BD FACSAria using ModFit LT 2.0 software. The experiment was repeated thrice.

Measurement of ruthenium(II) complexes -induced HeLa cell apoptosis: TUNEL staining is an effective method for finding early stage DNA fragmentation in apoptotic cells prior to changes in morphology. The blue channel represents DAPI-stained nuclei with an excitation wavelength of 340 nm. The red channel shows the luminescence of **2** with an excitation wavelength of 460 nm. The overlay

describes the cellular association of **2**. Briefly, HeLa cells cultured in 5% fetal bovine serum were treated with either vehicle or ruthenium(II) complex **2** (5, 20 μM) for 24 h. Afterwards, cell apoptosis was measured by terminal deoxynucleotide transferase dUTP nick end labelling (TUNEL) staining.[12] TUNEL staining was performed using an in situ cell death detection kit (Roche) according to the manufacturer's instructions. The number of TUNEL-positive cells was counted under a fluorescence microscope. Apoptotic and live cells were visualized with an inverted florescence microscope (Nikon, Tallahassee, Florida, USA) equipped with a CCD digital camera. Images were processed with image analysis software (NIS-Elements BR 3.0, Nikon, Tallahassee, Florida, USA).

Caspase activity: Harvested cells pellets were suspended in cell lysis buffer (Beyotime) and incubated on ice for 1 h. After centrifugation at 11,000 g for 30 min, supernatants were collected and immediately measured for protein concentration using BCA assay. Thereafter, a fluorometric method determined the caspase activity. In short, the cell lysates and specific caspase substrates (Ac-DEVD-AMC for caspase-3, Ac-IETD-AMC for caspase-8, and Ac-LEHD-AMC for caspase-9) were added into 96-well plates at 37 ℃ for 1 h. Fluorescence intensity was used to measure caspase activity with the excitation and emission wavelength set as 380 nm and 460 nm, respectively.

Determination of mitochondrial depolarization by flow cytometry: Mitochondrial transmembrane potential ($\Delta\psi_m$) was measured by measurement with 5,5',6,6'-tetrachloro-1,1',3,3'-tetraethyl-benzamidazolylcarbocyanine iodide (JC-1). After JC-1 staining, depolarization of the mitochondria was studied by monitoring the decrease in red fluorescence (JC-1 aggregates) and increase in green fluorescence (JC-1 monomers). The loss of $\Delta\Psi_m$ is correlated to a dose-dependent increase, as evidenced by the fluorescence shift of the JC-1 dye from red (~590 nm) to green (~525 nm).[13] HeLa cells were incubated with compound ruthenium(II) at concentrations (0, 5, 10, 20 μM) for 24 h. Cells were trypsinized, resuspended in 1 mL of PBS and incubated with 10 μg/mL JC-1 dye for 15 min. Both red and green fluorescence emissions were analyzed by flow cytometry using an excitation wavelength of 488 nm and observation wavelengths of 530 nm for green fluorescence and 585 nm for red fluorescence.

Detection of reactive oxygen species: There is also strong evidence supporting the idea that ROS are related to the induction of autophagy.[14] Treatment of HeLa cells with **1** and **2** were determined by using a fluorescent probe, 2',7'-dichlorofluorescein diacetate (H_2DCFDA). Non-fluorescent H_2DCFDA was oxidatively modified into a highly fluorescent derivative, 2,7-dichlorofluorescein (DCF), by intracellular ROS. As shown in Fig. 4A, HeLa cells were serially incubated with **1** and **2** at 0, 5, 10, and 20 μM for 24 h. Reactive oxygen species (ROS) generation was assessed as previously described by 2',7'-dichlorofluorescin diacetate (DCFH-DA), a lipid-permeable nonfluorescent compound that when oxidized by intracellular ROS forms the fluorescent compound 2',7'-dichlorofluorescein (DCF). HeLa cells were plated in phenol red-free RPMI containing 10 μmol/L DCFH-DA and treated with ruthenium(II) complexes. After 48 hours, the culture media and cells were collected. Cells were washed twice with PBS. The fluorescence of DCF in lysates and media was read in a black plate at 538 nm emission and 485 nm excitation and the values were standardized by lysate protein concentration. Negative controls containing dimethyl sulfoxide instead of DCFH-DA showed negligible fluorescence.

Figure Caption

Fig. S1 Emission spectral traces of complexes **1** (A) and **2** (B) in Tris/KCl buffer (100 mM KCl, 10 mM Tris HCl, pH 7.4) at increasing ratios of [Pu27]/[complex]= 0-10. [Complex] = 5 μM. (C) The relative fluorescence strength of complexes **1** and **2**. (D) Job plots resulting from the continuous variation analysis for complexes **1** and **2** with c-myc DNA in Tris–KCl buffer (100 mM KCl, 10 mM Tris–HCl, pH 7.4). These results are mean values of at least three independent experiments.

Fig. S2 (A) Effects of increasing amount (0-20 μM) complexes on the PCR. Complexes **1** and **2** on Pu27 in the PCR-stop assay. (B) The estimated IC_{50} (μM) values of complexes **1** and **2** based on the the PCR stop assay. These results are mean values of at least three independent experiments.

Fig. S3 FRET melting curves for experiments carried out with F27T (0.2 μM in 10 mM Tris-HCl 0.2 mM KCl, pH=7.4), at increasing concentrations of complexes **1** (A) and **2** (B). (C) Histogram of DNA melting temperatures ΔT_m disposed with Ru complex, r = [Ru]/[F27T]. Data were an average of three independent experiments and are presented as means ± standard deviations.

Fig. S4 Numbering of the c-myc sequences and proposed structures of the four different loop isomers and the corresponding proposed gel shift picture. The numbers of bases in each loop are 1:2:1 (G→T-14,23), 1:2:2 (G→T-14,20), 2:1:1 (G→T-11,23), and 2:1:2 (G→T-11,20), respectively.

Fig. S5 Emission titration of complexes **1** and **2** with four c-myc G-quadruplex loop isomers in Tris-KCl buffer, [Ru]=5 μM, [G-quadruplexes]=0-20 μM. Complex **1** interaction with the 2:1:1 loop isomer (A), the 1:2:2 loop isomer (B) and the 2:1:2 loop isomer (C). Complex **2** interaction with the 2:1:1 loop isomer (D), the 1:2:2 loop isomer (E) and the 2:1:2 loop isomer (F). These results are mean values of at least three independent experiments.

Fig. S6 (A) Relative fluorescence strength of complexes 1 and 2 with four c-myc G-quadruplex loop isomers. (B) The estimated IC_{50} (μM) values of complexes **1** and **2** on the four Pu18-mer loop isomers based on the the PCR stop assay. (C) Histogram of DNA melting temperatures ΔT_m disposed with complexes **1** and **2** on the four Pu18-mer loop isomers. Data were an average of three independent experiments and are presented as means ± standard deviations.

Fig. S7 Mean luminescence intensity of Hela cells incubated with complexes **1** and **2** for 12 h. Data were an average of three independent experiments and are presented as means ± standard deviations.

Fig. S8 (A) Analysis of caspase activity in complex **2**-induced apoptosis in HeLa cells. HeLa cells were treated with complex **2** for 72 h. Caspase activities were determined by synthetic fluorogenic substrate. (B) Cells were pretreated with 50 μM z-VAD-fmk, 100 μM z-IETD-

fmk, or 100 μM z-LEHD-fmk for 1 h, and then treated with complex **2** (10 μM for 6 h). DNA fragmentation was measured by DAPI staining. Data are presented as means ± SD of the results of three independent experiments.

Fig. S9 Changes of mitochondrial membrane potential in Hela cells incubated with complexes **1** and **2**. (A) Cells treated with different concentrations of complex were analyzed by JC-1 flow cytometry. (B) Cells treated with 20 μM complex at different time-courses were analyzed by JC-1 flow cytometry. Data were an average of three independent experiments and are presented as means ± standard deviations.

Fig. S10 Changes of ROS level in Hela cells incubated with complexes **1** and **2**. (A) Flow cytometrie analysis of cellular ROS level by DCFH-DA staining. (B) Relative intensity ratio of ROS with complexes under NAC. Data were an average of three independent experiments and are presented as means ± standard deviations.

Fig. S11 ESI-MS and ^{1}H-NMR spectra of complex $[Ru(bpy)_2(ODHIP)](ClO_4)_2$ (**1**).

Fig. S12 ESI-MS and ^{1}H-NMR spectra of complex $[Ru(phen)_2(ODHIP)](ClO_4)_2$ (**2**).

Scheme S1 Structure of $[Ru(bpy)_2(dhipH_3)](ClO_4)_2$ (**1**) and $[Ru(phen)_2(dhipH_3)](ClO_4)_2$ (**2**).

Table S1 Cytotoxic Effects of Ru Complexes towards different cell lines (IC_{50}, μM). These results are mean values of at least three independent experiments.

REFERENCES

1 Y. Xu, *Chem. Soc. Rev.*, 2011, **40**, 2719-2740.
2 Q. L. Zhang, J. H. Liu, X. Z. Ren, H. Xu, Y. Huang, J. Z. Liu and L. N. Ji, *J. Inorg. Biochem.*, 2003, **95**, 194-198.
3 G. L. Liao, X. Chen, L. N. Ji and H. Chao, *Chem. Commun.*, 2012, **48**, 10781-10783.
4 J. L. Yao, X. Gao, W. L. Sun, S. Shi and T. M. Yao, *Dalton Trans.*, 2013, **42**, 5661.
5 A. Ambrus, D. Chen, J. Dai, T. Bialis, R. A. Jones and D. Yang, *Nucleic Acids Res.*, 2006, **34**, 2723-2735.
6 C. Zhao, J. Geng, L. Feng, J. Ren and X. Qu, *Chem. Eur. J.*, 2011, **17**, 8209-8215.
7 A. De Cian, L. Guittat, M. Kaiser, B. Saccà, S. Amrane, A. Bourdoncle, P. Alberti, M.-P. Teulade-Fichou, L. Lacroix and J. L. Mergny, *Methods*, 2007, **42**, 183-195.
8 P. Wang, C. H. Leung, D. L. Ma, S. C. Yan and C. M. Che, *Chem. Eur. J.*, 2010, **16**, 6900-6911.
9 X. H. Zheng, H. Y. Chen, M. L. Tong, L. N. Ji and Z. W. Mao, *Chem. Commun.*, 2012, **48**, 7607-7609.
10 J. S.-Y. Lau, P. K. Lee, K. H.-K. Tsang, C. H.-C. Ng, Y. W. Lam, S. H. Cheng and K. K.-W. Lo, Inorg. Chem., 2008, **48**, 708-718.
11 C. Tan, S. Lai, S. Wu, S. Hu, L. Zhou, Y. Chen, M. Wang, Y. Zhu, W. Lian and W. Peng, *J. Med. Chem.*, 2010, **53**, 7613-7624.
12 W. Ruan, J. M. Xu, S. B. Li, L. Q. Yuan and R. P. Dai, *Cardiovasc. Res.*, 2012, **93**, 623-632.
13 G. J. Nowak, J. *Biol. Chem.*, 2002, **277**, 43377-43388.
14 R. Scherz-Shouval and Z. Elazar, *Trends Cell Biol*., 2007, **17**, 422-427.

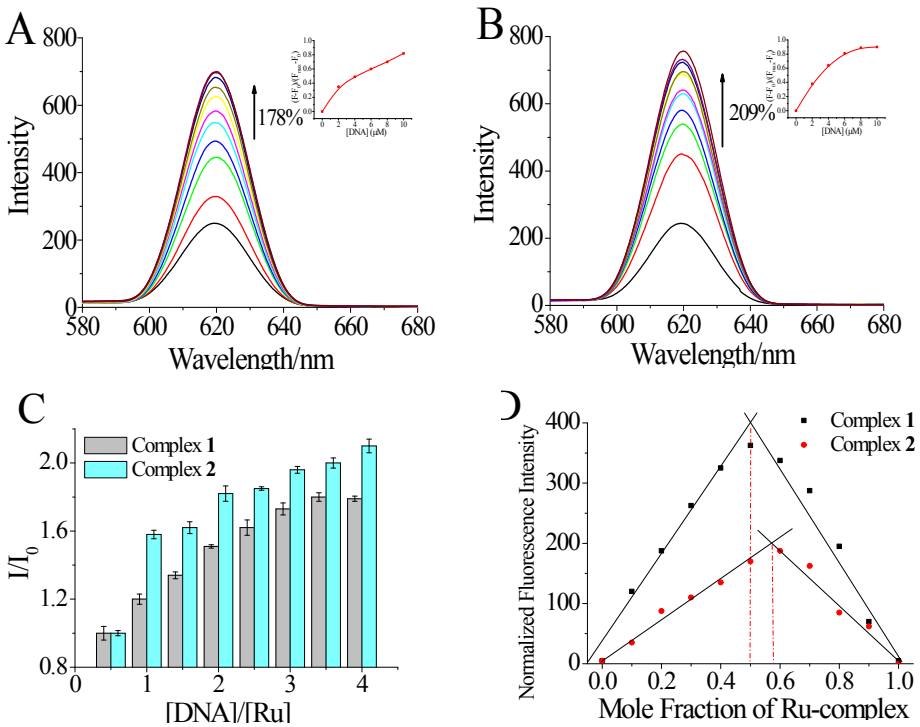

Fig. S1 Emission spectral traces of complexes **1** (A) and **2** (B) in Tris/KCl buffer (100 mM KCl, 10 mM Tris HCl, pH 7.4) at increasing ratios of [Pu27]/[complex]= 0-10. [Complex] = 5 μM. (C) The relative fluorescence strength of complexes 1 and 2. (D) Job plots resulting from the continuous variation analysis for complexes **1** and **2** with c-myc DNA in Tris–KCl buffer (100 mM KCl, 10 mM Tris–HCl, pH 7.4). These results are mean values of at least three independent experiments.

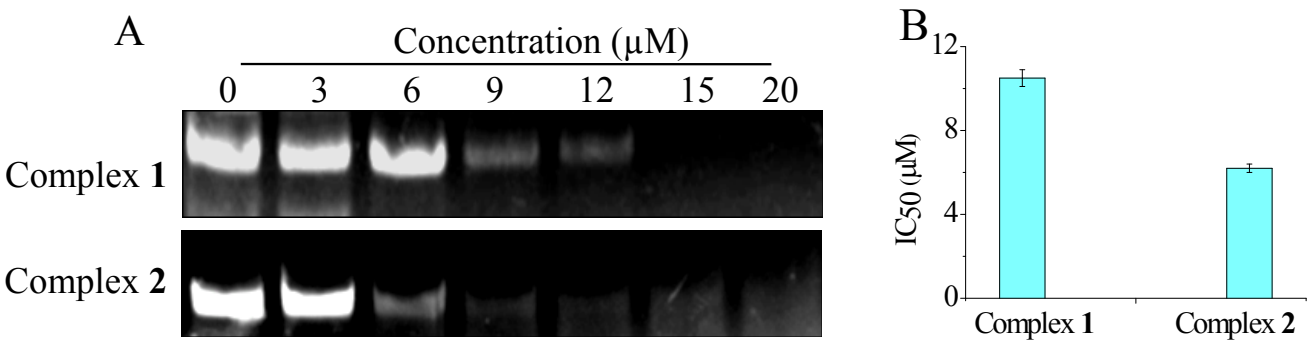

Fig. S2 (A) Effects of increasing amount (0-20 μM) complexes on the PCR. Complexes **1** and **2** on Pu27 in the PCR-stop assay. (B) The estimated IC_{50} (μM) values of complexes **1** and **2** based on the the PCR stop assay. These results are mean values of at least three independent experiments.

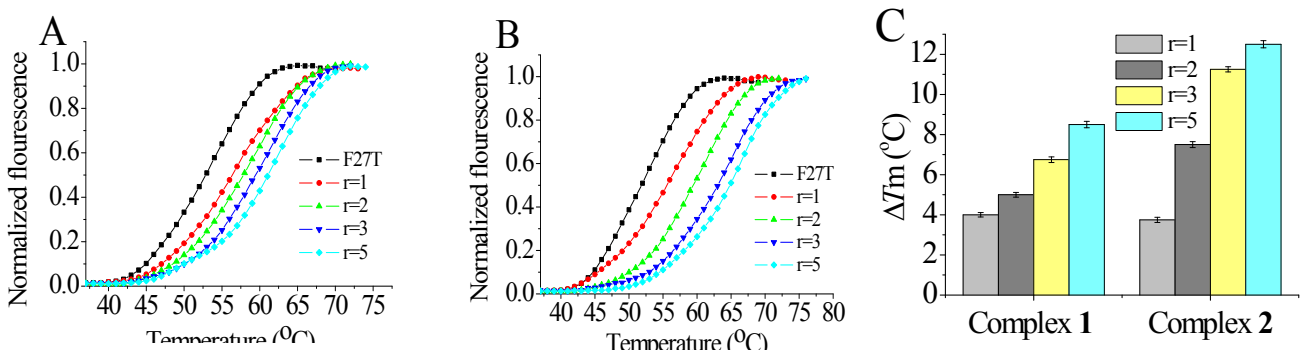

Fig. S3 FRET melting curves for experiments carried out with F27T (0.2 μM in 10 mM Tris-HCl 0.2 mM KCl, pH=7.4), at increasing concentrations of complexes **1** (A) and **2** (B). (C) Histogram of DNA melting temperatures ΔT_m disposed with Ru complex, r = [Ru]/[F27T]. Data were an average of three independent experiments and are presented as means ± standard deviations.

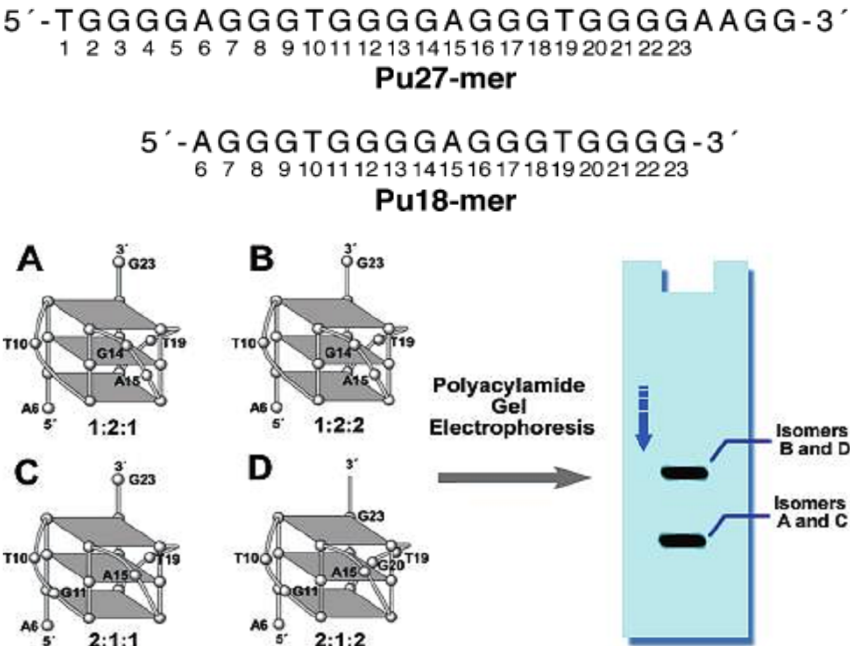

Fig. S4 Numbering of the c-myc sequences and proposed structures of the four different loop isomers and the corresponding proposed gel shift picture. The numbers of bases in each loop are 1:2:1 (G→T-14,23), 1:2:2 (G→T-14,20), 2:1:1 (G→T-11,23), and 2:1:2 (G→T-11,20), respectively.

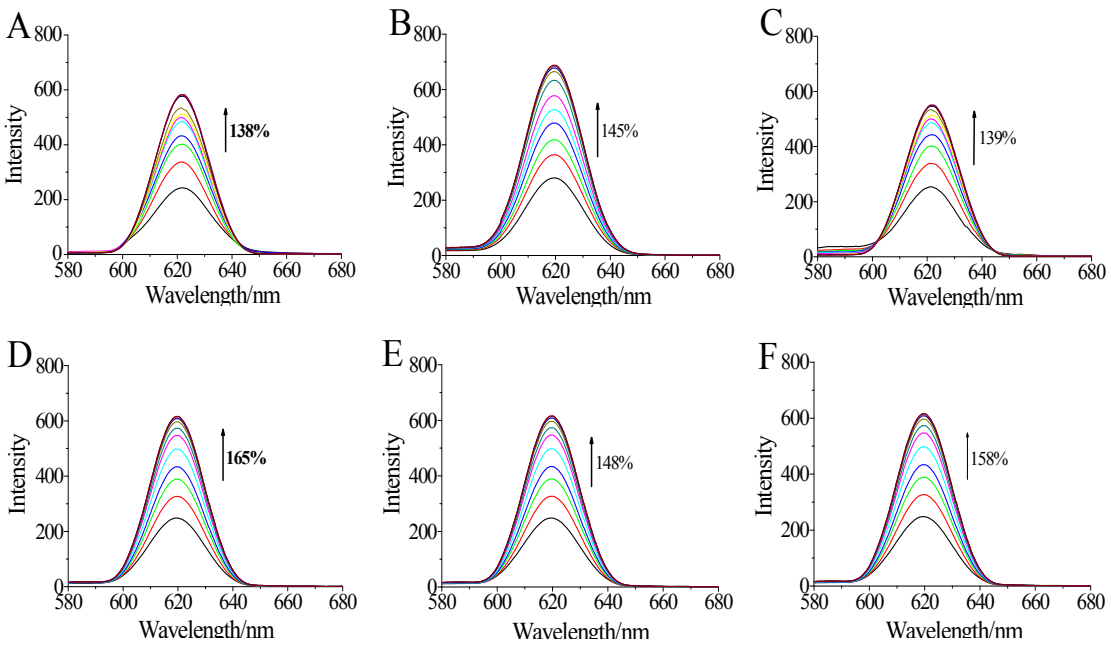

Fig. S5 Emission titration of complexes **1** and **2** with four c-myc G-quadruplex loop isomers in Tris-KCl buffer, [Ru]=5 μM, [G-quadruplexes]=0-20 μM. Complex **1** interaction with the 2:1:1 loop isomer (A), the 1:2:2 loop isomer (B) and the 2:1:2 loop isomer (C). Complex **2** interaction with the 2:1:1 loop isomer (D), the 1:2:2 loop isomer (E) and the 2:1:2 loop isomer (F). These results are mean values of at least three independent experiments.

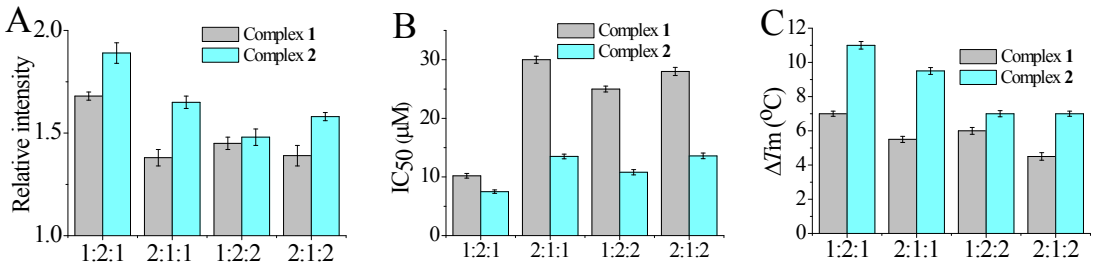

Fig. S6 (A) Relative fluorescence strength of complexes **1** and **2** with four c-myc G-quadruplex loop isomers. (B) The estimated IC_{50} (μM) values of complexes **1** and **2** on the four Pu18-mer loop isomers based on the the PCR stop assay. (C) Histogram of DNA melting temperatures ΔT_m disposed with complexes **1** and **2** on the four Pu18-mer loop isomers. Data were an average of three independent experiments and are presented as means ± standard deviations.

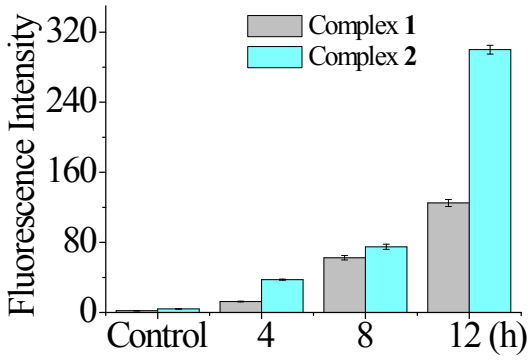

Fig. S7 Mean luminescence intensity of Hela cells incubated with complexes **1** and **2** for 12 h. Data were an average of three independent experiments and are presented as means ± standard deviations.

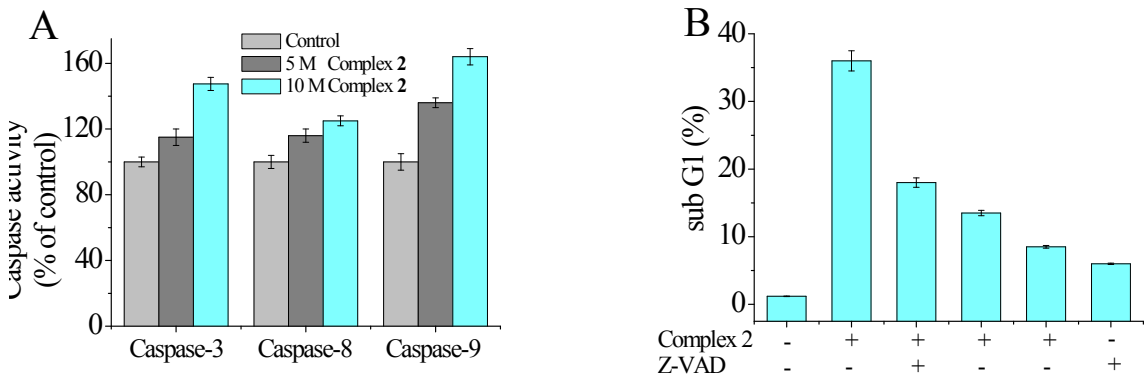

Fig. S8 (A) Analysis of caspase activity in complex **2**-induced apoptosis in HeLa cells. HeLa cells were treated with complex **2** for 72 h. (B) Cells were pretreated with 50 μM z-VAD-fmk, 100 μM z-IETD-fmk, or 100 μM z-LEHD-fmk for 1 h, and then treated with complex **2** (10 μM for 6 h). Data are presented as means ± SD of the results of three independent experiments.

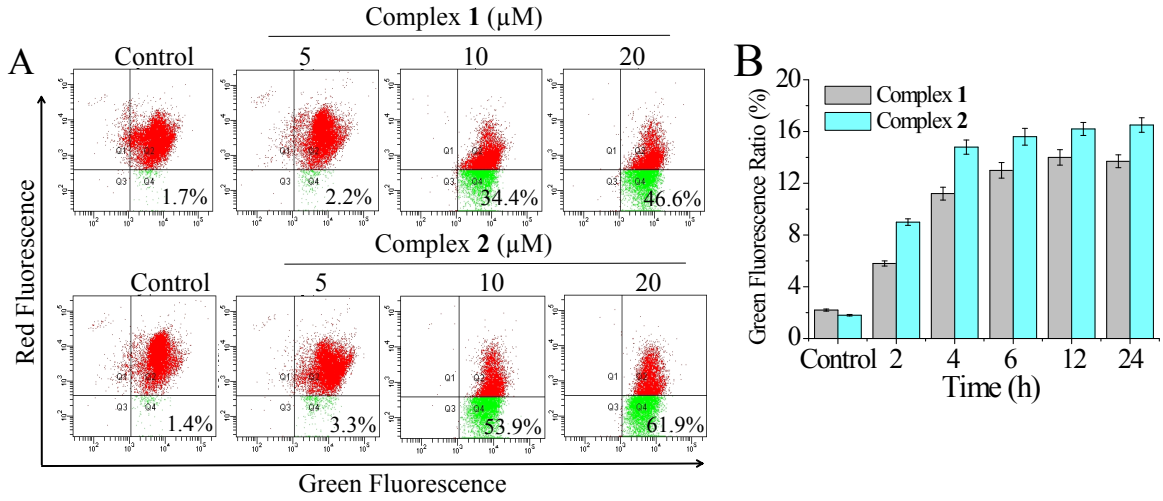

Fig. S9 Changes of mitochondrial membrane potential in Hela cells incubated with complexes **1** and **2**. (A) Cells treated with different concentrations of complex were analyzed by JC-1 flow cytometry. (B) Cells treated with 20 μM complex at different time-courses were analyzed by JC-1 flow cytometry. Data were an average of three independent experiments and are presented as means ± standard deviations.

Fig. S10 Changes of ROS level in Hela cells incubated with complexes **1** and **2**. (A) Flow cytometrie analysis of cellular ROS level by DCFH-DA staining. (B) Relative intensity ratio of ROS with complexes under NAC. Data were an average of three independent experiments and are presented as means ± standard deviations.

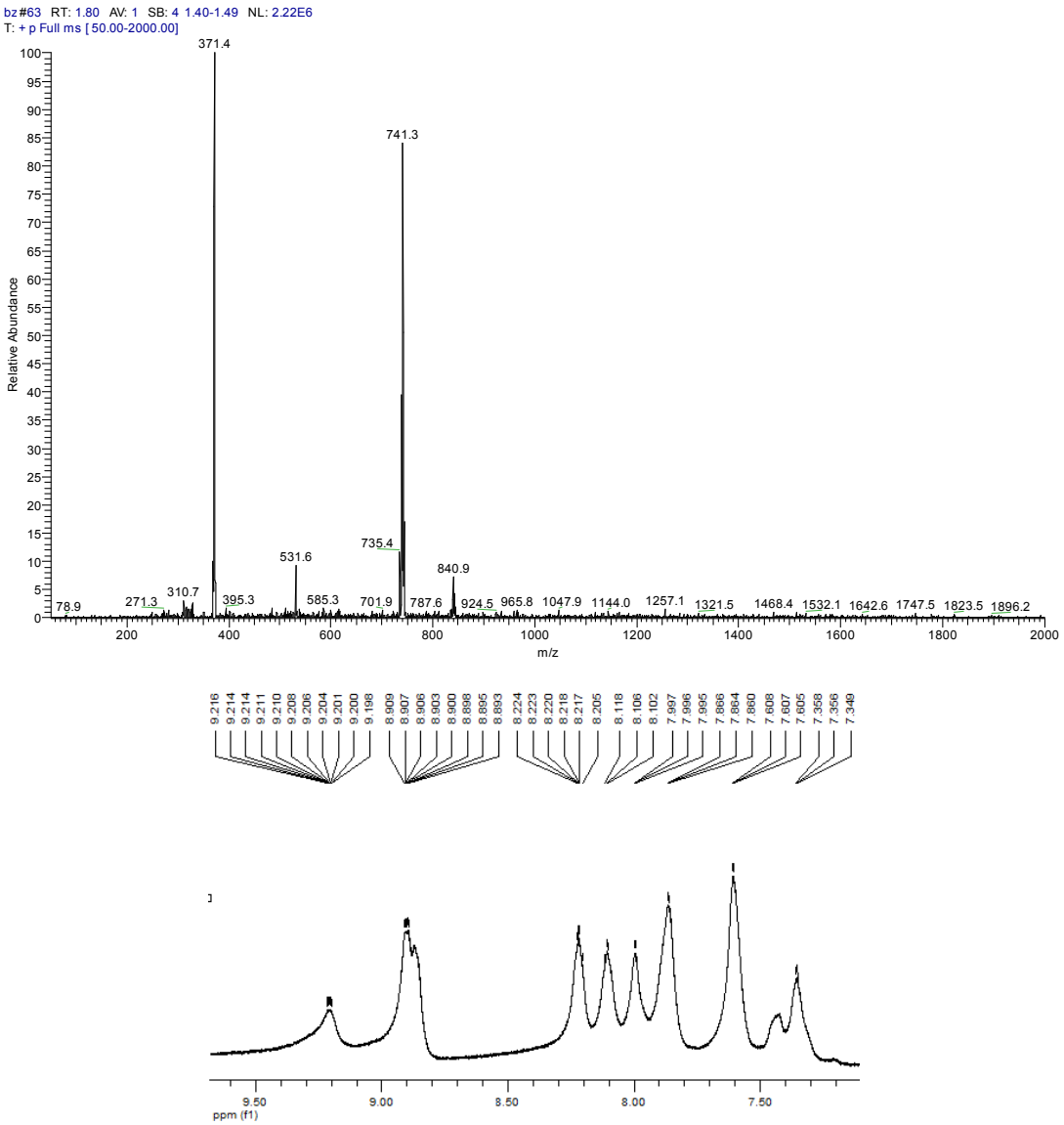

Fig. S11 ESI-MS and ^{1}H-NMR spectra of complex $[Ru(bpy)_2(ODHIP)](ClO_4)_2$ (**1**).

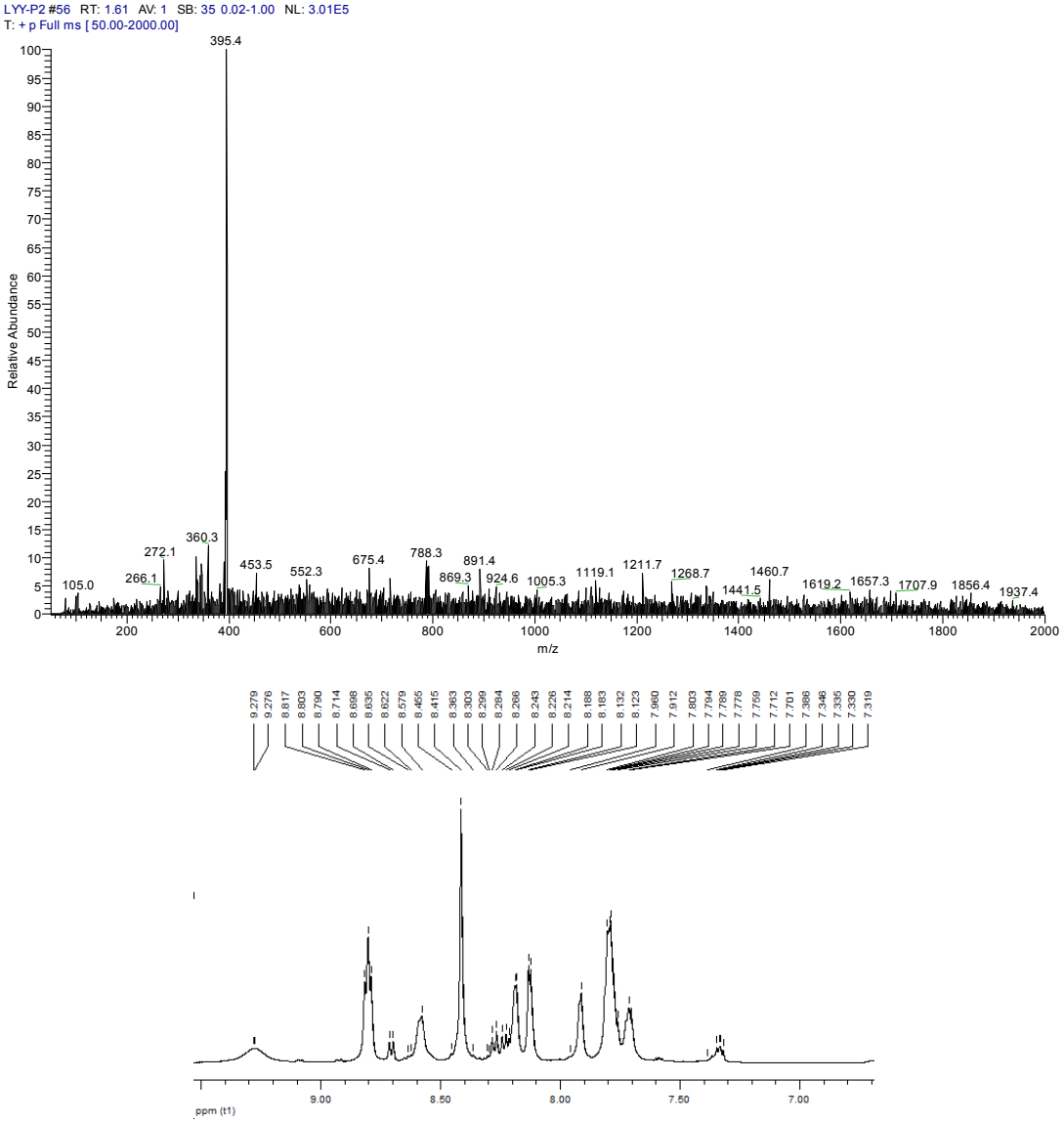

Fig. S12 ESI-MS and ^{1}H-NMR spectra of complex $[Ru(phen)_2(ODHIP)](ClO_4)_2$ (**2**).

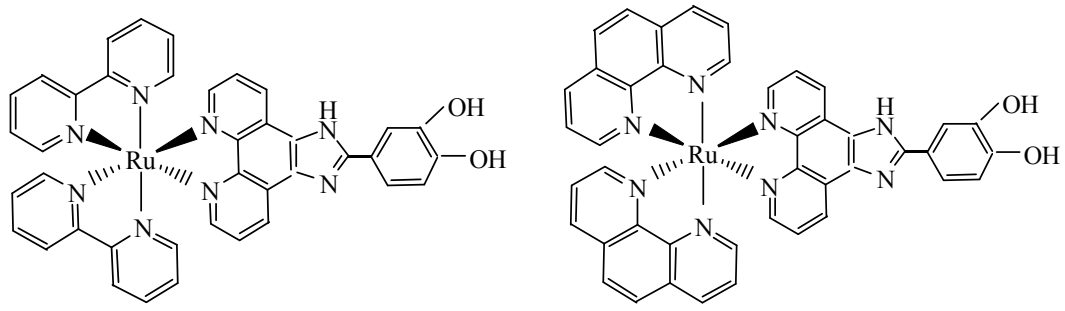

Complex **1** Complex **2**

Scheme S1. Structure of $[Ru(bpy)_2(dhipH_3)](ClO_4)_2$ (**1**) and $[Ru(phen)_2(dhipH_3)](ClO_4)_2$ (**2**).

Table S1. Cytotoxic Effects of Ru Complexes towards different cell lines (IC_{50}, μM). These results are mean values of at least three independent experiments.

Complex	Cytotoxicity (IC_{50}, μM)					
	Hela	HepG2	SW620	MCF-7	A459	Hs68
1	25.5 ± 1.1[#]	42.8 ± 3.4	83.0 ± 2.9	31.5 ± 0.9	71.7 ± 1.2	> 100
2	17.1 ± 2.4[*,#]	33.2 ± 2.7	61.5 ± 2.0	25.9 ± 1.2	50.8 ± 2.3	> 100
Cisplatin	22.3 ± 1.7	26.2 ± 2.1[*]	32.6 ± 1.4[*]	18.3 ± 0.9[*]	17.9 ± 1.0[*,#]	> 100

#, $P < 0.05$ in different cell lines; *, $P < 0.05$ in different complexes.